JOURNAL OF AIRCRAFT
Vol. 33, No. 2, March–April 1996

Numerical Model to Predict the Fate of Jettisoned Aviation Fuel

Karl D. Pfeiffer,* Dennis W. Quinn,† and Clifton E. Dungey‡
U.S. Air Force Institute of Technology, Wright–Patterson Air Force Base, Ohio 45433

While airborne, military and civilian aircraft must occasionally jettison unburned aviation fuel into the atmosphere. This research investigates the fate of jettisoned fuel (e.g., JP-4, JP-8, etc.) from initial release to final ground fall by numerically modeling the physical phenomena governing the fate of this fuel: evaporation, advection, and dispersion. Using previous work in evaporation and free fall of fuel droplets as a foundation, this article presents an integrated evaporation, advection, and dispersion model designed to run under the resources of a typical personal computer. This integrated model is capable of using near real-time meteorological data (i.e., vertical profiles of temperature, pressure, and wind) in all model calculations. Physical assumptions in the numerical model are presented, along with sample model calculations supporting these assumptions. Model calculations performed for two jettison scenarios show good agreement with previously published results and with an infinite line source calculation.

Nomenclature

C_d = droplet drag coefficient
c = point concentration
g = acceleration due to gravity, 9.81 m/s^2
K_x, K_y, K_z = dispersion coefficients along the x, y, and z axes
M_a = molecular weight of air, 28.96 kg/kmol
P = ambient pressure
Re = Reynolds number
R_0 = universal gas constant, 8314 (N·m)/(K·kmol)
r = droplet radius
T = ambient temperature
t = model time
U = mean wind speed, m/s
V = droplet air speed
V_{rel} = relative droplet speed, $U - V$
z = altitude
Γ = temperature lapse rate
Θ = time scale of the simulation
θ = mean wind direction
μ = kinematic viscosity of air
ρ = density of air
ρ_d = density of the fuel droplet
Σ_θ = total deviation of horizontal wind direction
σ_θ = observed deviation of the horizontal wind direction, rad
σ'_θ = deviation of the horizontal wind because of meteorological uncertainty
ϕ = release heading of aircraft

I. Introduction

WHILE airborne, military and civilian aircraft must occasionally jettison unburned aviation fuel into the atmosphere. This procedure is typically performed to reduce the weight of the aircraft, increasing the airworthiness of the aircraft and facilitating a safer landing (Ref. 1, p. 29). As early as 1959, Lowell developed a computer model to investigate the fate of jettisoned fuel.[2–4] His work established that jettisoning unburned fuel at most altitudes presented little or no flammability hazard. In the 1970s, the U.S. Air Force (USAF) began comprehensive research into the fate of jettisoned fuel, culminating in a series of technical reports by Clewell; in addition to investigating the frequency and nature of fuel jettison events within the USAF (Refs. 1 and 5), Clewell also investigated the evaporation and dispersion of JP-4 with a computer model.[6] Clewell used Lowell's work as a foundation, but incorporated more detail in the chemical model of JP-4 and in the simulation physics.[6,7] Clewell extended his own work with JP-4 by using the same model code to investigate the less volatile JP-8.[8] Clewell concluded that current (i.e., 1980) USAF minimum altitudes for fuel jettisoning (1500 m for tactical aircraft, 6000 m for strategic aircraft) resulted in a low threat of ground contamination by JP-4 over typical surface temperatures. Clewell found, however, that similar jettisoning events with JP-8 could cause some ground contamination, especially over colder surface temperatures.[9] The preliminary investigations of Lowell and Clewell provide detailed information about how much fuel will contaminate the ground after a particular jettison event. An open question remains: where will this fuel make ground fall? Quackenbush[10] recently investigated the question of ground-fall location for jettison events involving low airspeed, low altitude releases. Our work has resulted in a general model suited to high and medium altitude releases (6000–1500 m) at typical airspeeds for USAF aircraft. A further limitation to these previous studies is that a standard atmosphere was used for meteorological data. We incorporate near real-time weather data in our model to improve the prediction for both ground fall location and amount.

In this article we present a general model to assess the threat of ground contamination by an aviation fuel following a fuel jettison event. We incorporate previous work in fuel droplet evaporation[2,6] into an integrated evaporation, advection, and dispersion model; model output is a gridded data set of predicted concentration values, in either a grid-relative or map-relative coordinate system. We first present the model design and underlying physical assumptions. We then present several sample calculations from the model, comparing our results to previously published work and to a theoretical infinite line source calculation.

Received April 9, 1995; revision received Aug. 23, 1995; accepted for publication Oct. 3, 1995. This paper is declared a work of the U.S. Government and is not subject to copyright protection in the United States.

*Student, Department of Electrical and Computer Engineering, Graduate School of Engineering; currently Manager, Point Analysis Evaluation, U.S. Air Force Environmental and Technical Applications Center, 859 Buchanan Street, Scott Air Force Base, IL 62225.

†Professor of Mathematics, Graduate School of Engineering, 2950 P Street.

‡Assistant Professor of Atmospheric Physics, Graduate School of Engineering, 2950 P Street.

Our model code runs under the resources of a typical personal computer (e.g., i386 or i486 architecture), although it is portable enough to move easily to similar or more advanced architectures (e.g., DEC VAX or RISC workstations). The ANSI C source code, along with makefiles for common C compilers, are available via anonymous file-transfer protocol (FTP) at archive.afit.af.mil in the directory /pub/kpfeiffe.

II. Model Description

Lowell noted that determining the fate of jettisoned fuel requires characterizing many elusive physical phenomena, concluding that "... a completely general solution is merely a goal" (Ref. 2, p. 2). We approach our solution by decomposing the general problem into two smaller problems: 1) predicting the fate of an individual fuel droplet and 2) predicting the fate of the plume of jettisoned fuel. The fate of single fuel droplets is modeled with an evaporation and advection model calculating in a reference frame moving with the droplet. The fate of the plume is modeled with a dispersion model calculating in a reference frame moving with the plume. Model calculations are supported by an environmental model that provides meteorological data at altitude from the point of jettison to final ground fall.

A. Physical Assumptions

In coupling the evaporation results to the dispersion model, we assume the jettisoned plume is a monodisperse system; that is, we assume the plume consists of a continuous distribution of fuel droplets, all of the same diameter. Clewell found good agreement between evaporation model predictions for a single droplet at mass median diameter for a KC-135 (270 μm) and other distributions of droplets. His conclusion was that "the central tendency ... of the droplet sizes is relatively unimportant for determining the composite evaporation and free fall of the distribution" (Ref. 6, p. 60).

We assume that the initial plume of jettisoned fuel is created by an aircraft flying at fixed speed, altitude, and heading, using a constant release rate. A review of Clewell's record of USAF jettison events[5] suggests that these assumptions are reasonable; typically, we will not have better information with which to formulate initial conditions. Of these assumptions, perhaps the least representative is that the initial plume is a single straight line. Clewell reported that a typical dumping pattern, called a racetrack, involves a 2-min downwind leg, a 2-min turn, a 2-min upwind leg, and another 2-min turn (Ref. 1, p. 34). We argue that we could simulate a racetrack as a series of four or more straight segments, each segment used as an initial condition to a complete model run.

We assume not only that our plume is straight, but also that the plume begins at a single altitude. This is equivalent to assuming that the plume is jettisoned instantaneously. This simplification causes acceptably small errors in calculating plume length both at the initial release and at ground fall. Modifications to the model code to investigate this error showed an upper bound of less than 10^{-4}, or 0.01% of the total plume length (Ref. 11, Sec. 4.4).

Immediately upon jettison the plume of fuel is under the influence of the aircraft wake. We do not attempt to model any of the physical forces in the wake. Rather, we consider only the net effect in spreading the initial plume; that is, we assume a particular initial width of plume associated with a particular aircraft or jettison configuration. Clewell neglected wake effects in the free fall and evaporation model, noting that this underestimates initial droplet terminal velocities; that is, the wake tends to push the plume down (Ref. 6, pp. 38, 39). From experimental results, Clewell concluded that this underestimate resulted in an error of about 100 m in altitude in the overall descent (Ref. 6, p. 43).

B. Meteorological Model

1. *Meteorological Model Description*

We treat the atmosphere as a table of meteorological attributes ordered by altitude. Attributes necessary to model calculations are pressure, temperature, wind speed and direction, density, and viscosity. Upon receiving a query for data at z, the model searches the table for observations z_{low} and z_{high} such that $z_{low} \leq z \leq z_{high}$. If z is identical to an observation in the table, that observation is used to return the queried attribute; otherwise the attribute at z is interpolated from data at z_{low} and z_{high}.

2. *Meteorological Model Initialization*

Ideally, the model is initialized with radiosonde data, commonly referred to as upper air data. Several hundred stations worldwide collect upper air data daily at 0000 and 1200 UTC (Ref. 12, p. 17) [UTC is Universal Time Code; it is also known as Greenwich Mean Time (GMT)]. These reports, along with other current meteorological data, are commonly available over public communication networks; Ahlquist[13] provides an extensive review of meteorological data available over the Internet. Ancillary to the model code, we created a utility, getmet, to facilitate creating model-ready atmospheric data files from the raw, teletype upper air data available on the Internet. The source code for this utility is available via anonymous FTP at archive.afit.af.mil. Because previous work uses a standard atmosphere uniformly warmed or cooled based on surface temperature, we also produced a utility, makestd, to create model-ready atmospheric data files based on the standard atmosphere and a supplied surface temperature. Source code for this utility is also available via anonymous FTP.

3. *Meteorological Model Physics*

Pressure, temperature, and wind are treated as observations in the table. Density and viscosity are calculated on demand.

To interpolate T at z between observations at z_{low} and z_{high}, we first compute Γ using

$$\Gamma = -\left(\frac{T_{high} - T_{low}}{z_{high} - z_{low}}\right) \tag{1}$$

T is interpolated with the simple linear rule:

$$T = T_{low} - \Gamma(z - z_{low}) \tag{2}$$

Pressure P at z is interpolated using a form of the scale height equation for a hydrostatically balanced atmosphere (Ref. 14, p. 83):

$$P = P_{low}(T/T_{low})^{gM_a/(\Gamma R_0)} \tag{3}$$

We note that this relation may not recover P_{high} if the hydrostatic assumption is poor; however, we always satisfy $P_{low} \geq P \geq P_{high}$. If the layer is isothermal (i.e., $\Gamma = 0$), P is calculated using a simple linear interpolation between P_{low} and P_{high}.

Wind speed and direction are decomposed into two components: 1) an E–W zonal component and 2) a N–S meridional component. Component wind speed at altitude is interpolated using a simple linear relation similar to Eq. (2).

Density ρ is calculated assuming air is an ideal gas. Kinematic viscosity μ is calculated using a relation published in the *U.S. Standard Atmosphere* (Ref. 15, p. 7):

$$\mu = \frac{1.458 \times 10^{-6} T}{110.4 + T} \tag{4}$$

where T is assumed to be in Kelvin. The units of μ for this relation are $kg \cdot m^{-1}s^{-1}$.

C. Evaporation and Advection (E/A) Model

1. E/A Model Description

The evaporation and advection model follows the droplet in time, space, physical dimensions, and chemical composition. Because we have defined a jettison to last from release to ground fall or evaporation, this model component also determines Θ.

We approach the advection of the plume of jettisoned fuel by examining the advection of individual droplets. We assume that a droplet begins with the velocity of the jettisoning aircraft and decelerates into the mean wind flow. This assumption may be very poor for an individual droplet in the plume; turbulent eddies about the mean wind flow will drive a single particle in a random walk about the center of the plume. For the average of a large number of particles, however, this is a good assumption; in fact, this is the basis of Lagrangian dispersion modeling (see, e.g., Zannetti,[16] Chap. 8). We treat dispersion separately, however, and so we accept that our advection model is in fact following the ensemble-averaged position of this particle, which should correspond to the c.m. of the plume (Ref. 17, pp. 532–534).

We employ an aggressive time step scheme, similar to previous work[4,6]; however, we present the details of our application of this adaptive method for the sake of clarity. Each iteration of the model begins with an estimated time step Δt. In calculating the changes in altitude Δz, latitude Δy, and longitude Δx, the model algorithm alters this Δt if Δx, Δy, or Δz calculations exceed threshold distances (nominally 100 m). These constraints on the growth of the time step are necessary to maintain the integrity of our piecewise linear approximations to the nonlinear changes in droplet mass and terminal velocity. The algorithms controlling mass and temperature calculations can also alter Δt, if necessary, to bring these heat and mass losses to within threshold. At the end of the cycle, Δt is doubled and submitted as the first guess for the next iteration. Typical model results reported by Clewell show a time step that increases to the order of tens of minutes near the end of model execution (Ref. 6, pp. 108–118). This model accounts for both droplet descent and horizontal translation; wind speed is typically on the order of 10 m/s (Ref. 18, pp. 120, 121), whereas the droplet terminal velocity is initially on the order of 1 m/s (Ref. 6, p. 108). Higher wind speeds increase the horizontal displacement of the droplet and cause the model algorithm to reduce Δt and slow model execution noticeably.

We extend previous work in free fall and evaporation by incorporating representative meteorology into droplet descent. Both Lowell and Clewell reported their results in terms of surface temperatures; colder surface temperatures resulted in less evaporation and more ground contamination, warmer surface temperatures resulted in more evaporation and less ground contamination. Using only a standard atmosphere uniformly warmed or cooled to the surface, this approach is insensitive to temperature inversions and other temperature anomalies along the droplet's path of descent. Through the atmosphere, air temperature normally decreases with height; temperature inversions are areas where air temperature increases with height [for a brief discussion of inversions, see Wark and Warner (Ref. 19, pp. 80, 81)]. In the reference frame on the droplet, passing through an inversion slows down the evaporation rate as the droplet cools on descent. Evaporation calculations over an inversion layer will necessarily yield a different prediction from calculations performed using a standard atmosphere. We present results in Sec. III that support this assertion.

2. E/A Model Initialization

Model calculations assume the droplet has an initial chemical composition (e.g., Clewell's 33-component JP-4), an initial altitude equal to the release height of the aircraft, and an initial temperature corresponding to the stagnation, or equilibrium, temperature of the droplet with respect to the aircraft fuel tank [see, e.g., Holman (Ref. 20, pp. 173, 174)]. This treatment is consistent with Clewell (Ref. 6, p. 87). The droplet position is assumed to be the midpoint of the jettisoned plume, calculated based on the reported latitude, longitude, airspeed, and heading of the aircraft at the start of the fuel jettison.

3. E/A Model Physics

Evaporation calculations follow the work developed by Lowell[2,4] and extended by Clewell.[6] Specific adaptations for our integrated model are presented by Pfeiffer.[11]

We treat horizontal droplet motion using two-dimensional rectangular coordinates aligned meridionally (N–S) and zonally (E–W). We assume the droplet begins with the speed of the jettisoning aircraft and decelerates into the mean wind. To model the droplets in two dimensions, we perform a one-dimensional analysis, then generalize the results to two dimensions. Starting with Newton's second law and assuming the only external force on the droplet is drag, we arrive at the differential equation for V (Ref. 11, Sec. 3.5.3.2):

$$\frac{dV}{dt} = \frac{3\rho}{8\rho_d r} C_d (U - V)^2 \tag{5}$$

Because the droplet has initial airspeed V_0 at $t = 0$, we have

$$\int_{V_0}^{V} \frac{dV}{(U - V)^2} = \int_0^t \frac{3\rho}{8\rho_d r} C_d \, dt \tag{6}$$

If we further assume that C_d, ρ, ρ_d, and r are constant, integration yields

$$V = U - \frac{U - V_0}{1 + \frac{3}{8}(\rho/\rho_d)(1/r)C_d(U - V_0)^2 t} \tag{7}$$

Equation (7) has the property that $V \to U$ as $t \to \infty$, which fits our original intuition that the droplet decelerates into the mean flow.

The droplet drag coefficient is a function of Re of the flow. Bilanin[21] and Teske[22] suggest a relationship between Re and C_d for spherical droplets, originally developed by Langmuir and Blodgett:

$$C_d = (24/Re)(1 + 0.197Re^{0.63} + 2.6 \times 10^{-4} Re^{1.38}) \tag{8}$$

Examining the order of magnitude of terms in Eq. (7) does not suggest that we can neglect this initial deceleration. Model results suggest a deceleration time typically on the order of seconds (Ref. 11, pp. 4-7–4-10).

Once in the mean flow, droplet trajectory is computed using the component wind speeds and Δt. We account for Coriolis accelerations in the droplet trajectory by assuming the droplet follows the wind.

D. Dispersion Model

1. Dispersion Model Description

We treat the plume of jettisoned fuel as a continuous mass distributed over a horizontal plane. The plume is modeled over a two-dimensional grid that extends beyond the physical dimension of the plume, so that there always exists a zero-concentration boundary condition on the grid. The two-dimensional diffusion equation, Eq. (10), is solved numerically over this grid for a given time Θ using time step Δt. This Δt is independent of the time step used in the evaporation and advection model.

The grid is initialized with a fixed mass at $t = 0$, then updated at intervals of Δt; Δt may be fixed or variable, depending on the numerical scheme. After each iteration, the plume dimension is examined with respect to the grid dimension, and if the solution appears to be creeping to the edges of the grid, the grid is expanded in place. This expansion does not add points to the grid, but rather doubles the step size between grid

points. The current grid is embedded in a new grid nominally twice the dimension of the current grid, and so the zero-concentration boundary condition is maintained. Execution continues until $t = \Theta$.

2. Dispersion Model Initialization

The grid is initialized with a plume of known mass, length and width where length is assumed to be the dominant horizontal dimension. For convenience, the plume length is aligned on the x axis, while plume width is aligned on the y axis.

Plume mass is distributed in a line along the y axis so that the resulting concentration along the line has a Gaussian distribution

$$g(y) = \begin{cases} \dfrac{1}{\sigma\sqrt{2\pi}} \exp\left[\dfrac{-(y - y_0)^2}{2\sigma^2}\right] & \text{for} \quad 0 < |y - y_0| < L_y \\ 0 & \text{for} \quad |y - y_0| > L_y \end{cases} \tag{9}$$

where y_0 is the coordinate of the center of the plume, L_y is the length of the plume, and $\sigma = L_y/3$. We adjust σ to reduce the size of the jump discontinuity at the edges of the plume. Distribution along the x axis is uniform over most of the plume length, with short (approximately 10% of plume length) ramp-up and ramp-down distributions at the ends of the plume. These adjustments to the ends of the plume are made to facilitate a smoother numerical solution; similarly, the assumption of a Gaussian distribution along the plume width is convenient. Although we do not have experimental evidence to formulate precisely these initial conditions, we do know qualitatively that we can consider our plume as a line source. Our Gaussian initial conditions are consistent with steady-state, continuous source solutions for a line source [see, e.g., Seinfeld (Ref. 17, p. 600) or Hanna (Ref. 23, pp. 51, 52)]. We conclude that our initial conditions are representative of the initial release and distribution of the aviation fuel.

3. Dispersion Model Physics

We model the distribution of concentration over the grid using a simplified form of the Fickian or K-theory diffusion equation [see, e.g., Seinfeld (Ref. 17, p. 522) or Zannetti (Ref. 16, p. 107)]:

$$\frac{\partial c}{\partial t} = K_x \frac{\partial^2 c}{\partial x^2} + K_y \frac{\partial^2 c}{\partial y^2} \tag{10}$$

where c is the ensemble-averaged or mean concentration and K_x and K_y are the eddy diffusion coefficients. This treatment assumes that molecular diffusion is negligible and that the primary mechanism affecting concentration is atmospheric turbulence, parameterized in K_x and K_y (Ref. 17, pp. 522, 523). We conclude that c is not affected by changes in mass and so we are justified in treating dispersion separately from evaporation. Advection, often incorporated into the diffusion equation, is already considered in a separate model. Strikwerda, in particular, has demonstrated that advection and dispersion in a fixed reference frame are equivalent to dispersion in an advected reference frame (Ref. 24, p. 114).

We are interested in the deposition concentration (mass per area) at ground fall. We deliberately chose a two-dimensional reference frame for our plume, assuming that vertical dispersion is negligible and that, similar to our advection model, our plane is located through the c.m. of the plume (Ref. 17, p. 534). We assume, then, that when the droplet makes ground fall the plume strikes the ground; that is, all mass in the column above the droplet simultaneously makes ground fall.

To calculate a numerical solution to Eq. (10) we adapt a Fourier series solution to our grid in a method similar to an analytical derivation presented by Seinfeld (Ref. 17, p. 553). To verify results from this Fourier technique, we also implement a finite difference solution, described by Pfeiffer (Ref. 11, Sec. 3.6.4.3).

4. Numerical Method

We begin with Eq. (10) and assume boundary and initial conditions:

$$c(x, y, 0) = p(x)q(y)$$

$$c(x, 0, t) = c(x, L_y, t) = 0 \quad \text{for} \quad 0 \le x \le L_x, \; t > 0$$

$$c(0, y, t) = c(L_x, y, t) = 0 \quad \text{for} \quad 0 \le y \le L_y, \; t > 0$$

where L_x is the plume length. The initial condition implies that the initial distribution is separable in x and y. We assume further that we can separate $c(x, y, t)$ into $c = f(x, t)g(y, t)$, so that Eq. (10) becomes two partial differential equations (PDEs). We continue analysis with $f(x, t)$ and note its similarity to $g(y, t)$. The PDE in f is

$$\frac{\partial f}{\partial t} - K_x \frac{\partial^2 f}{\partial x^2} = 0 \tag{11}$$

where

$$f(x, 0) = p(x)$$

$$f(0, t) = f(L_x, t) = 0 \quad \text{for} \quad t > 0$$

If f satisfies Eq. (11) and g satisfies a similar equation, and $c = fg$, then c satisfies Eq. (10). By the uniqueness theorem for the diffusion equation this is the only solution [for a brief discussion see Sommerfeld (Ref. 25, pp. 82, 83) or Arfken (Ref. 26, p. 79)].

The Fourier series solution of Eq. (11) is

$$f(x, t) = \sum_{n=1}^{\infty} A_n \sin\left(\frac{n\pi x}{L}\right) \exp\left(\frac{-K_x n^2 \pi^2}{L^2} t\right) \tag{12}$$

where

$$A_n = \frac{2}{L} \int_0^L p(x) \sin \frac{n\pi x}{L} \, dx \tag{13}$$

This is a common result [see, e.g., Burden and Faires (Ref. 27, pp. 566, 567) or Boas (Ref. 28, pp. 543–547)]. We could calculate our solution directly with this treatment, setting $t = \Theta$, the total time of descent, to arrive at the concentration distribution at the ground. We can only calculate a finite number of terms, however, and with Θ on the order of 1–10 h, we would have to include an excessively large number of Fourier terms to get a reasonably accurate solution. Such a one-step solution is particularly bad if the physical plume grows to exceed L at $t = \Theta$, because this situation violates zero boundary conditions. To make certain that our model matches the physical plume we incorporate this Fourier solution into an iterative scheme.

The iterative solution uses m time steps such that $\Theta = m\Delta t$, where Δt is chosen empirically as a compromise between accuracy and time. At each time step, new Fourier coefficients (nominally 60–80) are calculated using the trapezoid rule to integrate Eq. (13) over the grid, and so the previous time step's $f(x)$ becomes the following time step's $p(x)$.

Zero-concentration boundary conditions are initialized by embedding the plume dimension d (referring either to width or length) in the center of a grid line of dimension $3 \cdot d$. These boundary conditions are maintained by examining solution creep after every iteration. Solution creep is determined by

comparing plume dimension to grid length. Plume dimension is defined to be the line that contains the set of all concentration values greater than $0.001 f_{max}$ where f_{max} is the maximum concentration in the plume line. The threshold, set empirically, is plume dimension grid line length $> \frac{2}{3}$. That is, if the plume dimension has crept to two-thirds of the grid line, the grid must be expanded in place to maintain zero boundary conditions.

5. Eddy Diffusion Parameters

Implicit in our numerical solution is a scheme to calculate the eddy diffusion coefficients K_x and K_y. Zannetti (Ref. 16, pp. 125–130), Seinfeld (Ref. 17, pp. 597, 598), and Hanna (Ref. 23, pp. 50–56) present extensive discussions on calculating horizontal diffusion parameters for specific solutions to Eq. (10) and the general advection–diffusion equation.

Eddy diffusion is typically parameterized in terms of conveniently measured (or estimated) quantities (Ref. 23, p. 27). We have wind and temperature data along the droplet descent from the meteorological model. From this data we can infer the variability of the wind, then approximate the eddy turbulence parameters K_x and K_y. Zannetti offers the following relation for long-range transport and diffusion from a point source for an arbitrary horizontal dispersion parameter K_h (Ref. 16, p. 128):

$$K_h = 10^3 \sigma_\theta^2 U/2 \tag{14}$$

Zannetti (Ref. 16, p. 128) develops Eq. (14) based on work by Irwin. Hanna (Ref. 23, p. 31) presents a similar result with reference to Irwin. Zannetti notes that this relation results in dispersion parameters an order to two orders of magnitude smaller than the low end of the range of experimentally derived parameters [10^2–10^3 vs 10^4–10^7 m^2/s (Ref. 16, p. 128)]. Experimentally derived parameters, however, necessarily incorporate the variability of measurements; Zannetti accounts for the anomalously small K_h from Eq. (14) in the uncertainty of the meteorological diagnosis or prognosis of the wind field (Ref. 16, p. 128). In examining uncertainty in air quality models, Lewellen[29] used an estimate of uncertainty in rawinsonde wind measurements that varied from ±5 deg at 10 m/s to ±180 deg under calm conditions. We take the observed deviation in wind direction as σ_θ, and take the deviation in wind direction due to meteorological uncertainty as σ'_θ. Using Lewellen's uncertainty estimation, we fit an exponential function for σ'_θ over the range of wind speeds less than 10 m/s, so that

$$\sigma'_\theta = \pi \exp(-0.367U) \tag{15}$$

where we expect U in meters per second and return σ'_θ in radians. Finally, we substitute into Eq. (14) the term Σ_θ for σ_θ, where

$$\Sigma_\theta = \sigma_\theta + \sigma'_\theta \tag{16}$$

With a single vertical profile, we cannot directly calculate σ_θ; we approximate this quantity at altitude z by examining the variability of the wind through a layer centered (vertically) at z. The x axis is, by design, along the release heading of the aircraft ϕ, and so the y axis must be along the heading ϕ + 90 deg. If we define θ to be the mean wind direction at altitude, our eddy diffusion parameters are

$$K_x = [10^3 \Sigma_\theta^2 U |\cos(\phi - \theta)|]/2 \tag{17}$$

$$K_y = [10^3 \Sigma_\theta^2 U |\cos(90 \text{ deg} - \phi - \theta)|]/2 \tag{18}$$

III. Model Results and Sample Calculations

We now present results from the implementation of our integrated model. We noted in Sec. II.C that using a standard atmosphere assumption in evaporation calculations could lead to errors in predicted ground fall. We present results from two case studies that demonstrate these errors and the utility of using representative meteorological data in model calculations. We then present sample calculations from the integrated model, comparing our results to results in Clewell[6] and a line source calculation developed in this research.

A. Representative Meteorology

We introduce representative meteorology into the integrated model by means of the passive environmental model. Although we did not perform an exhaustive study of the effect of different meteorological conditions on the overall simulation, we present sample cases that demonstrate the utility of this model. We conducted a brief study using upper air data from Spokane, Washington, for Oct. 1, 1994, 0000 UTC, and Dayton, Ohio, for Oct. 1, 1994, 1200 UTC. We compared these actual temperature profiles to adjusted standard atmospheres at the same surface temperatures. We used a release altitude of 1500 m and an airspeed of 175 m/s to generate results for JP-4 and JP-8. Consistent with our integrated model we assumed a mean diameter of 270 μm. Because we do not have a standard wind profile in the same sense that we have a standard atmosphere, we limit our comparison to the differing temperature profiles and the resulting differences in liquid fuel ground fall.

Spokane, WA: The Spokane data show a suface temperature of 21.4°C; we created a standard atmosphere profile adjusted to this temperature using the makestd utility (see Sec. II.B). The actual and standard temperature profiles are detailed in Fig. 1. We see that the actual temperature profile at Spokane is much warmer than the standard profile throughout the layer from 1500 m to surface. Evaporation results are detailed in Table 1. We observe that for the relatively volatile JP-4 this warmer temperature profile does not significantly effect the amount of fuel making ground fall. We surmise that the general state of the atmosphere is relatively warm, and so the JP-4 evaporates readily in both profiles. For JP-8 we observe an order-of-magnitude difference between predicted ground fall from a standard atmosphere (2.11%) and the actual profile (0.15%).

Table 1 Predicted percentage ground fall from Spokane and Dayton studies

	Spokane		Dayton	
Fuel	Actual profile	Standard profile	Actual profile	Standard profile
JP-4	0.10	0.13	0.09	0.17
JP-8	0.15	2.11	0.15	8.50

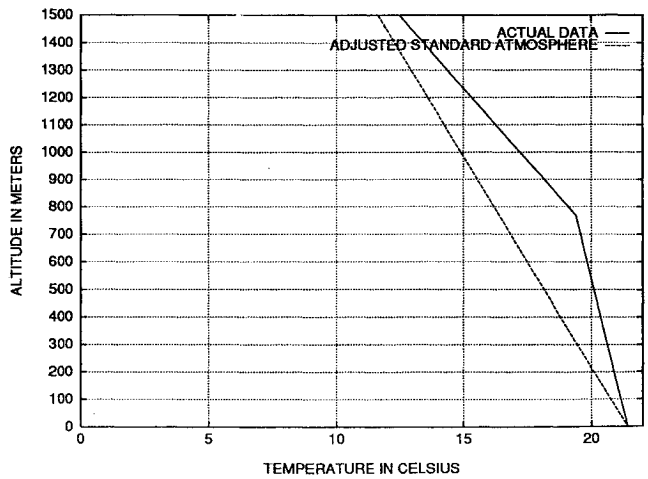

Fig. 1 Spokane (Oct. 1, 94/0000 UTC) and standard profile.

Dayton, OH: The profile at Dayton on Oct. 1, 1994, 1200 UTC, shows a deep surface inversion approximately 450 m in depth (see Fig. 2). With this inversion, the actual profile is much warmer than the standard profile. Consistent with the Spokane study, we find that the predicted ground fall for JP-4 is only mildly affected by the differences in temperature profiles. Calculations with JP-8 using the standard profile, however, overpredicted ground fall by almost two orders of magnitude, 8.5% in contrast to the actual profile prediction of 0.15%. Ground-fall predictions are summarized in Table 1. Figure 3 shows the descent history for the Dayton JP-8 case.

Although we do not examine advection in this study, we do note that predicted time to ground fall increased under the warmer temperature profiles. These results are presented in Table 2. The large differences in predicted ground-fall times for JP-4 and JP-8 represent significant periods (10^3–10^4 s) over which the fuel droplets will continue to advect and disperse. While two case studies are hardly exhaustive, these cases suggest that large errors in predicted ground contamination are possible if no consideration is given to representative meteorology. From our results, however, these errors seem to be conservative, significantly overestimating ground contamination from liquid fuel.

B. Sample Calculations from the Integrated Model

We now present sample calculations from the integrated model, following a simulation from release to final ground fall with detailed model output on location and concentration of the remaining liquid fuel. For these sample calculations, we use the iterative Fourier method described in Sec. II.D, with the initial data modeled with a Gaussian ramp-up along the plume length.

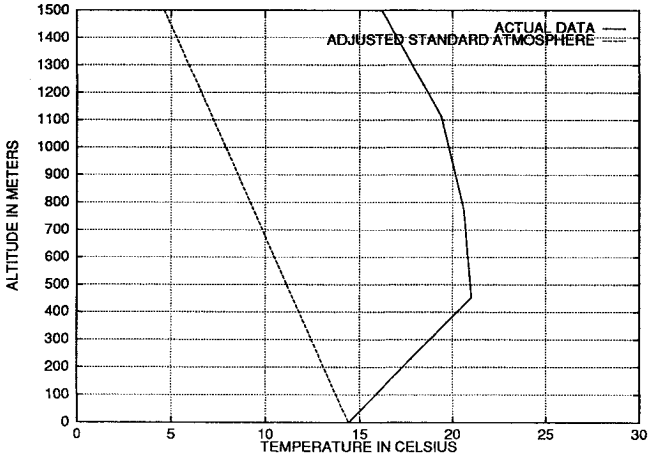

Fig. 2 Dayton (Oct. 1, 94/1200 UTC) and standard profile.

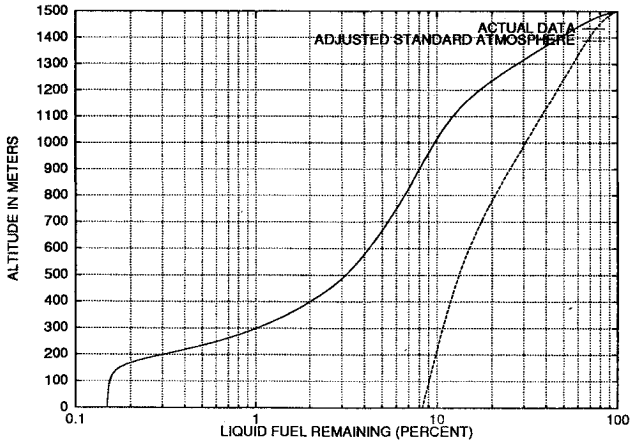

Fig. 3 Dayton study, JP-8 ground fall.

Clewell made several calculations for maximum ground contamination using a simple box model (Ref. 6, pp. 73–75). This calculation spreads an infinite line source over the width of the plume at the time of maximum ground contamination. We note that this box model uses an infinite line source because there is no time-like variable for duration of release.

We compare Clewell's results with two calculations performed with the integrated model, a typical KC-135 jettison and a typical F-111 jettison. Typical values are based on Clewell's summary and analysis of USAF jettison reports.[1,5] Comparisons with Clewell's results demonstrate that our model results are physically meaningful. To demonstrate that our model is numerically sound, we examine our model results compared to an infinite line source calculation.

1. *Case 1: Example KC-135 Release*

We first examined a KC-135 release with the following attributes: release airspeed 175 m/s, jettison rate 50 kg/s, release height 6 km, initial plume width 100 m, ground-level temperature −20°C, and wind from 270 deg at 4 m/s. We assumed a duration of 5 min, typical for the KC-135 based on USAF fuel jettison reports.[1,5] Consistent with Clewell, we examined both downwind (parallel to the mean wind) releases and crosswind (perpendicular to the mean wind) releases. For reference, we started the jettison over latitude 39.54 (N) and longitude −84.12 (W). Results are summarized and compared to the box model calculations in Table 3.

For the downwind release, the aircraft heading was taken as 270 deg, while for the crosswind release the aircraft heading was taken as 180 deg. Figures 4 and 5 show the grid-relative results for the downwind and crosswind release for case 1. Consistent with our intuition, the downwind release (Fig. 4) maintains a line source character as ground fall because of preferential dispersion along the plume length. Similarly, the crosswind release (Fig. 5) looks like an area source because of preferential dispersion along the plume width. The model produces both grid-relative and map-relative output; however, we present the map-relative output for the crosswind release of case 1 in Fig. 6.

We observe that our predicted maximum concentrations (extracted from the gridded model output) are about an order of magnitude larger than Clewell's box model predictions. To explain this difference, we examine y axis (plume width) cross sections in Figs. 7 and 8. Although we predict a higher maximum concentration, we claim that the box model calculation

Table 2 Ground-fall times (in minutes) from Spokane and Dayton studies

	Spokane		Dayton	
Fuel	Actual profile	Standard profile	Actual profile	Standard profile
JP-4	819.7	728.9	918.5	503.4
JP-8	130.7	78.7	212.8	54.8

Table 3 Comparison of results for case 1

	Clewell	Iterated Fourier
Downwind		
Peak contamination, kg/m^2	2.7×10^{-7}	6.2×10^{-6}
Plume width, km	90	0.9
Cross section contaminants, kg/m	0.024	0.022
Crosswind		
Peak contamination, kg/m^2	7.0×10^{-8}	1.9×10^{-6}
Plume width, km	330	2.6
Cross section contaminants, kg/m	0.023	0.023

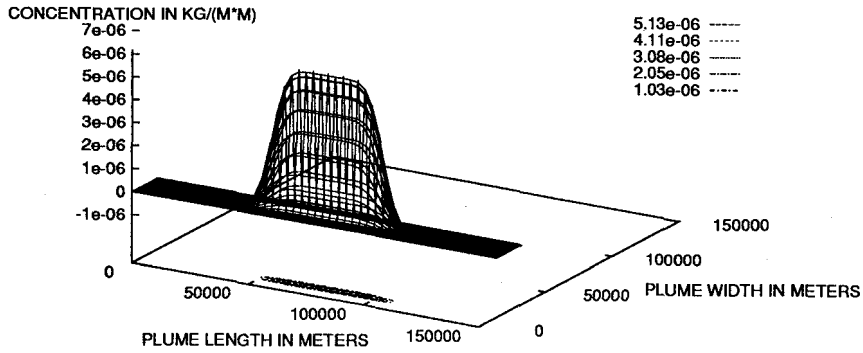

Fig. 4 Grid-relative output for case 1, downwind release.

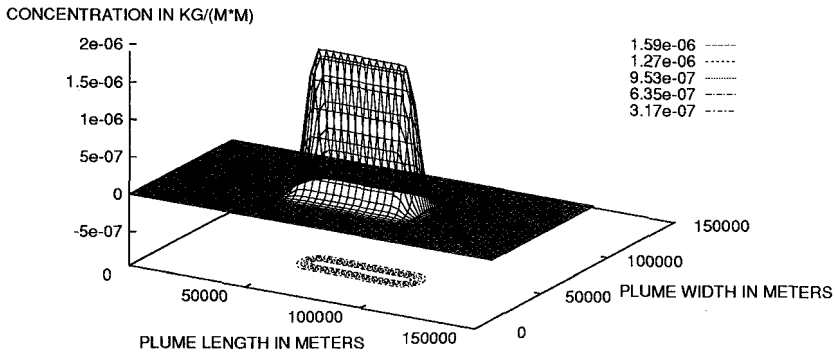

Fig. 5 Grid-relative output for case 1, crosswind release.

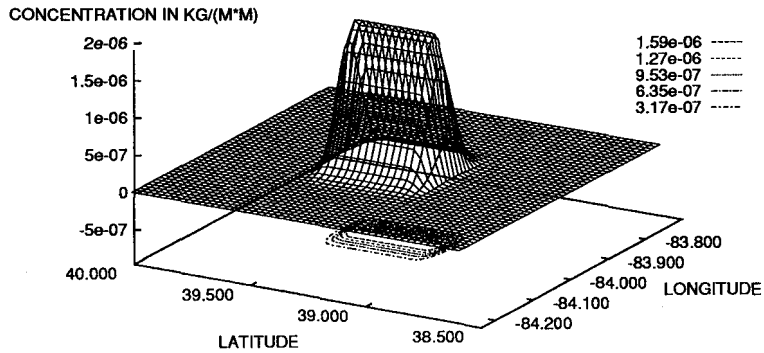

Fig. 6 Map-relative output for case 1, crosswind release.

is dispersing the same amount of material in a less conservative manner. To support our assertion, Table 3 contains cross section contaminations (in kilograms per meter). This is calculated for Clewell's results by multiplying the plume width by the peak (and only) concentration. Our model reports this quantity by integrating along the y axis at the midpoint of the x axis. We observe close agreement between cross section concentrations; however, our model yields a significant improvement in assessing the largest point contamination areas (i.e., along the centerline).

In Clewell, plume width refers to the physical dimension of the single maximum concentration isopleth at the ground (Ref. 6, p. 74). To compare our results, we defined plume width to be the distance across the plume within which all concentration values greater than or equal to 95% of the maximum (centerline) concentration fall.

2. *Case 2: Example F-111 Release*

We examined an F-111 jettison with the following attributes: release airspeed 175 m/s, jettison rate 17 kg/s, release height 1.5 km, initial plume width 20 m, ground-level temperature 0°C, and wind from 270 deg at 5 m/s. We assumed a duration of 2 min, again consistent with Clewell's earlier work.[1,5] As in case 1, we examine both downwind and crosswind releases with headings of 270 and 180 deg, respectively.

Results are summarized in Table 4. As in case 1, we predict higher peak concentrations than those predicted by the box model. Cross sections in Figs. 9 and 10 show, however, that our model calculations and the box model calculations are dispersing the same mass (see Table 4). For case 2 our predictions are 2–3 times larger than the box model predictions vs the 25–30 times larger predictions for case 1. We suspect that we have a closer agreement in case 2 with the box model because our distribution at the ground is more box-like (i.e., the edges of the plume are sharper) than case 1. We note that the case 1 descent is 173 min, whereas the case 2 descent is 132 min; case 1 has a longer time to disperse. Further, case 2 has a higher wind speed (5 m/s vs 4 m/s), which results in a smaller Σ_θ (628 m^2/s vs 1048 m^2/s) in the direction of the wind.

3. *Infinite Line Source Calculation*

To further verify our results, we derive an infinite line source

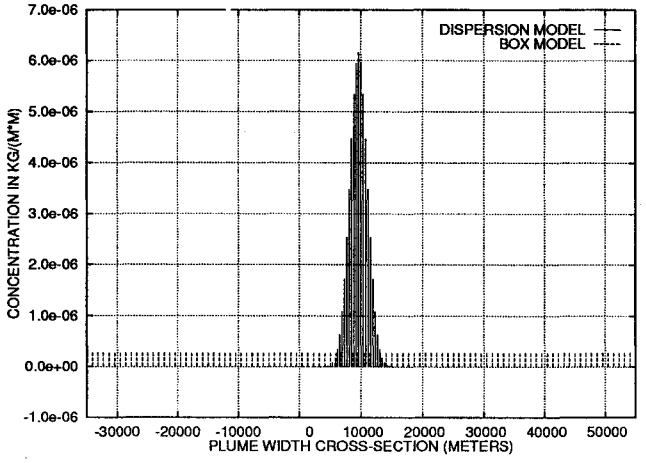

Fig. 7 Cross section of the plume width for case 1, downwind release.

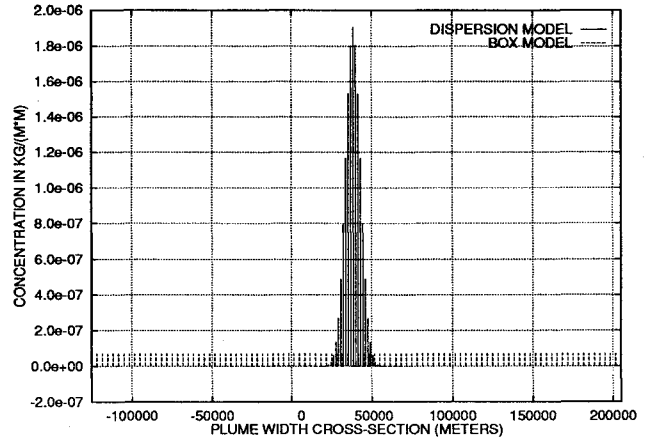

Fig. 8 Cross section of the plume width for case 1, crosswind release.

calculation. We begin with the three-dimensional diffusion equation (Ref. 17, p. 535):

$$\frac{\partial c}{\partial t} = K_x \frac{\partial^2 c}{\partial x^2} + K_y \frac{\partial^2 c}{\partial y^2} + K_z \frac{\partial^2 c}{\partial z^2} \tag{19}$$

For an instantaneous point source at (x_0, y_0, z_0), with constant diffusivity parameters and source strength Q, this has the analytic solution (Ref. 23, p. 51):

$$c(x, y, z, t) = \frac{Q}{(4\pi t)^{3/2}(K_x K_y K_z)^{1/2}} \times \exp\left[-\frac{(x - x_0)^2}{4K_x t} - \frac{(y - y_0)^2}{4K_y t} - \frac{(z - z_0)^2}{4K_z t}\right] \tag{20}$$

To derive an analytic solution for an infinite line source coincident with the x axis, we take Q^* to be the line source strength and integrate Eq. (20) along x from $-\infty$ to ∞. This approach is similar to Lowell (Ref. 3, p. 7). We assume that all of the material in the vertical column over a point in the xy plane strike the ground simultaneously. To reflect this in our line source calculation, we integrate along the z axis from $-\infty$ to ∞,

$$c(y, t) = \int_{-\infty}^{\infty} \frac{Q^*}{4\pi t(K_y K_z)^{1/2}} \exp\left[-\frac{(y - y_0)^2}{4K_y t} - \frac{(z - z_0)^2}{4K_z t}\right] dz \tag{21}$$

Table 4 Comparison of results for case 2

	Clewell	Iterated Fourier
Downwind		
Peak contaminants, kg/m^2	2.8×10^{-7}	5.5×10^{-7}
Plume width, km	5	0.7
Cross section contaminants, kg/m	0.0014	0.0017
Crosswind		
Peak contaminants, kg/m^2	8.0×10^{-8}	2.2×10^{-7}
Plume width, km	19	1.8
Cross section contaminants, kg/m	0.0015	0.0017

and arrive at

$$c(y, t) = \frac{Q^*}{2(\pi K_y t)^{1/2}} \exp\left[-\frac{(y - y_0)^2}{4K_y t}\right] \tag{22}$$

We note that if Q^* has dimension of mass per unit length, our expression for $c(y, t)$ has dimension of mass per unit area, consistent with our model calculations. If we consider only the maximum concentration in the context of Eq. (22), this maximum is necessarily on the centerline, at $y = y_0$, so that,

$$c(t) = \frac{Q^*}{2(\pi K_y t)^{1/2}} \tag{23}$$

Using this equation as an estimator for maximum concentration, we revisit our model results for the KC-135 release and the F-111 short-duration (case 2) release. Results are summarized in Table 5.

We consider the original line source strength at release Q^* and multiply this number by the mass fraction remaining at ground fall. The form of Eq. (23) is such that at $t = 0$, $c(t)$ is infinite. Clearly our model does not start with these initial conditions; we always assume a finite initial concentration distribution. For case 1, our initial maximum centerline concentration is $c_0 = 1.55 \times 10^{-3}$ kg/m^2. For case 2, our initial maximum centerline concentration is $c_0 = 1.66 \times 10^{-3}$ kg/m^2. We rearrange Eq. (23) to calculate the time at which our model initial condition c_0 is valid:

$$t = (1/4\pi K_y)(Q^*/c_0)^2 \tag{24}$$

The largest value for t in the cases considered is for the downwind release in case 1, resulting in $t = 27$ s. The time scale Θ of these cases is on the order of 10^3–10^4 s (see Table 5). We assume, then, that the theoretical line source quickly evolves into the area source we use as an initial condition for the model. Thus, the times used in Table 5 are the times of descent of the droplets.

Table 5 shows that our model is in close agreement with the infinite line source calculation. From this agreement we conclude that our model is numerically sound. We note that this infinite line source calculation uses the same K_y derived in Sec. II.D. We do not claim that these results reinforce the physical character of our model; both calculations (dispersion model and infinite line source) rely on the empirically determined diffusion coefficients. We do note that the iterative Fourier solution and the derived line source calculation [Eq. (22)] solve exactly the same differential equation and should have very nearly the same solution for $t > 3$ s near the center of the plume (where we are examining the maximum concentrations).

Given that this infinite line source calculation appears to be in good agreement with our model results, we might ask: why not use the source calculation? Our sample calculations are necessarily simple cases, with constant wind profiles, and hence, constant diffusion coefficients. More realistic problems

Table 5 Comparison of model results with linear source calculation

	Q^*, kg/m	Fraction	K_y, m²/s	t, s	Model results, kg/m²	Line source, kg/m²
Case 1						
Downwind	0.286	0.078	100	10,368	6.2×10^{-6}	6.2×10^{-6}
Crosswind	0.286	0.078	1,048	10,368	1.9×10^{-6}	1.9×10^{-6}
Case 2						
Downwind	0.097	0.018	100	7,920	5.5×10^{-7}	5.5×10^{-7}
Crosswind	0.097	0.018	628	7,920	2.2×10^{-7}	2.1×10^{-7}

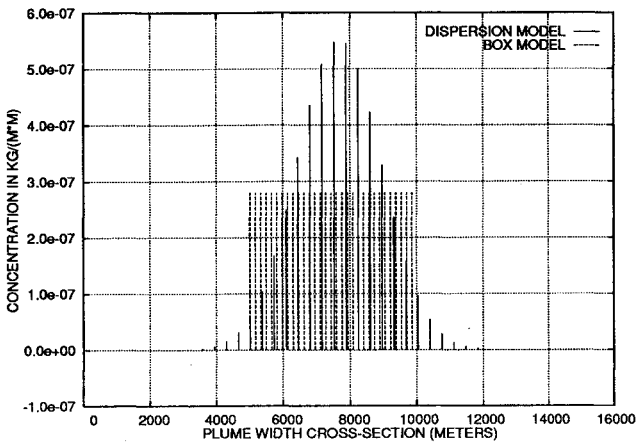

Fig. 9 Cross section of the plume width for case 2, downwind release.

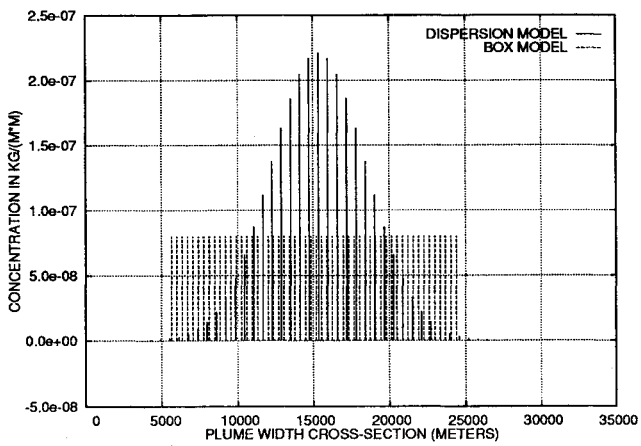

Fig. 10 Cross section of the plume width for case 2, crosswind release.

using actual meteorological observations could not be treated so simply. Further, we cannot get a good sense of the complete plume dimension with the infinite line source; by assumption the length along the release path is infinite. The computational complexity introduced in our model is necessary, then, to calculate complete information about ground contamination.

Overall, we found good agreement between maximum concentration results from our model calculations and from Clewell's box model as well with our infinite line source calculation.

IV. Summary

Aircraft in flight must occasionally jettison unburned aviation fuel into the atmosphere. A body of literature exists to determine how much of this unburned fuel may contaminate the ground; however, little work has been accomplished to determine the transport and dispersion of this material.

Our goal in this research was to develop a general tool for predicting the fate of jettisoned aviation fuel. We have successfully designed and implemented an evaporation, advection, and dispersion model capable of predicting ground-fall location and concentration of an aviation fuel following a fuel jettison event. We have demonstrated that our calculations produce physically meaningful results, in reasonable agreement with previously published work. In designing our model, we have improved previous work in droplet evaporation by incorporating near real-time meteorological information. In brief case studies, we have demonstrated that this data can significantly improve model predictions.

While we have verified that model calculations are correct, we have only briefly touched on the investigations possible with our general tool. We have shown that meteorological conditions are potentially significant in the evaporation (and consequently, the advection and dispersion) of jettisoned fuel. Given the availability of weather data over the Internet and through other public sources, many location-specific and climate-specific studies are possible. These kinds of studies may be useful in assessing long-term effects of repeated fuel jettisoning in a geographic region.

We have limited our studies to the aviation fuels JP-4 and JP-8, and have limited our calculations to descent and ground fall of liquid fuel. Although studies of jet fuel–soil interactions have been reported in the literature (see, e.g., Dean-Ross,[30,31]), these studies typically deal with the liquid fuel in its original form. We know at ground fall, however, that our contaminant has a significantly different chemical character. This model, then, could be applied as a first step in studies of soil and watershed contamination from jettisoned fuel, similar to studies in pesticide spray and dispersion models.[32–34] Further, this model is capable of using any aviation fuel. Other fuels, especially newer or broadened-specification fuels, would make useful studies both to improve knowledge about potential ground contamination and to improve knowledge about the model.

The eddy diffusion parameters within the model are currently based on order-of-magnitude estimates using wind speed and wind variation. Significant improvement to the model physics could be made with a study and calibration of these coefficients.

References

[1]Clewell, H. J., "Fuel Jettisoning by U.S. Air Force Aircraft, Volume I: Summary and Analysis," Air Force Engineering and Services Center, ESL-TR-80-17, AD-A089010, Tyndall AFB, FL, March 1980.

[2]Lowell, H. H., "Free Fall and Evaporation of JP-4 Fuel Droplets in a Quiet Atmosphere," NASA TN D-33, Washington, DC, Sept. 1959.

[3]Lowell, H. H., "Dispersion of Jettisoned JP-4 Jet Fuel by Atmospheric Turbulence, Evaporation, and Varying Rates of Fall of Fuel Droplets," NASA TN D-84, Washington, DC, Oct. 1959.

[4]Lowell, H. H., "Free Fall and Evaporation of JP-1 Jet Fuel Droplets in a Quiet Atmosphere," NASA TN D-199, Washington, DC, March 1960.

[5]Clewell, H. J., "Fuel Jettisoning by U.S. Air Force Aircraft, Volume II: Fuel Dump Listings," Air Force Engineering and Services Center, ESL-TR-80-17, AD-A089076, Tyndall AFB, FL, March 1980.

[6]Clewell, H. J., "Evaporation and Groundfall of JP-4 Jet Fuel Jettisoned by USAF Aircraft," Air Force Engineering and Services Cen-

ter, ESL-TR-80-56, AD-A109307, Tyndall AFB, FL, Sept. 1980.

[7]Good, R. E., and Clewell, H. J., "Drop Formation and Evaporation of JP-4 Fuel Jettisoned from Aircraft," *Journal of Aircraft*, Vol. 17, No. 7, 1980, pp. 450–456.

[8]Clewell, H. J., "The Effect of Fuel Composition on Groundfall from Aircraft Fuel Jettisoning," Air Force Engineering and Services Center, ESL-TR-81-13, AD-A110305, Tyndall AFB, FL, March 1981.

[9]Clewell, H. J., "Ground Contamination by Fuel Jettisoned from Aircraft in Flight," *Journal of Aircraft*, Vol. 20, No. 3, 1983, pp. 382–384.

[10]Quackenbush, T. R., and Teske, M. E., "A Model for Assessing Fuel Jettisoning Effects," *Atmospheric Environment*, Vol. 28, Oct. 1994, pp. 2751–2759.

[11]Pfeiffer, K. D., "A Numerical Model to Determine the Fate of Jettisoned Aviation Fuel," M.S. Thesis, School of Engineering, Air Force Inst. of Technology, Wright–Patterson AFB, OH, Dec. 1994.

[12]Henderson-Sellers, A., and Robinson, P. J., *Contemporary Climatology*, Longman Scientific and Technical, Essex, England, UK, 1986.

[13]Ahlquist, J., "Free Software and Information via Computer Network," *Bulletin of the American Meteorological Society*, Vol. 74, March 1993, pp. 377–386.

[14]Hess, S. L., *Introduction to Theoretical Meteorology*, Krieger, Malabar, FL, 1959.

[15]*U.S. Standard Atmosphere, 1976*, U.S. Committee on Extension to the Standard Atmosphere, Washington: National Oceanic and Atmospheric Administration, 1976.

[16]Zannetti, P., *Air Pollution Modeling: Theories, Computational Methods, and Available Software*, Reinhold, New York, 1990.

[17]Seinfeld, J. H., *Atmospheric Chemistry and Physics of Air Pollution*, Wiley, New York, 1986.

[18]Holton, J. R., *Introduction to Dynamic Meteorology*, 2nd ed., Academic, Orlando, FL, 1979.

[19]Wark, K., and Warner, C. F., *Air Pollution: Its Origin and Control*, Harper Collins Publishers, New York, 1981.

[20]Holman, J., *Heat Transfer*, 5th ed., McGraw–Hill, New York, 1981.

[21]Bilanin, A. J., Teske, M. E., Barry, J. W., and Ekblad, R. B., "Agdisp: The Aircraft Spray Dispersion Model, Code Development and Experimental Validation," *Transactions of the American Society of Agricultural Engineers*, Vol. 32, Jan.–Feb. 1989, pp. 327–334.

[22]Teske, M. E., Bowers, J. F., Rafferty, J. E., and Barry, J. W., "FSCBG: An Aerial Spray Dispersion Model for Predicting the Fate of Released Material Behind Aircraft," *Environmental Toxicology and Chemistry*, Vol. 12, No. 3, 1993, pp. 453–464.

[23]Hanna, S. R., Briggs, G. A., and Hosker, R. P., Jr., *Handbook on Atmospheric Diffusion*, Technical Information Center, U.S. Dept. of Energy, DOE/TIC-11223, 1982.

[24]Strikwerda, J. C., *Finite Difference Schemes and Partial Differential Equations*, Wadsworth and Brooks, Pacific Grove, CA, 1989.

[25]Sommerfeld, A., *Partial Differential Equations in Physics*, Academic, New York, 1949.

[26]Arfken, G., *Mathematical Methods for Physicists*, 3rd ed., Academic, Orlando, FL, 1985.

[27]Burden, R. L., and Faires, J. D., *Numerical Analysis*, 3rd ed., Prindle, Weber, and Schmidt, Boston, MA, 1985.

[28]Boas, M. L., *Mathematical Methods in the Physical Sciences*, Wiley, New York, 1983.

[29]Lewellan, W., and Sykes, R., "Meteorological Data Needs for Modeling Air Quality Uncertainties," *Journal of Atmospheric and Oceanic Technology*, Vol. 6, Oct. 1989, pp. 759–768.

[30]Dean-Ross, D., Mayfield, H., and Spain, J., "Environmental Fate and Effects of Jet Fuel JP-8," *Chemosphere*, Vol. 24, Jan. 1992, pp. 219–228.

[31]Dean-Ross, D., "Fate of Jet Fuel JP-4 in Soil," *Bulletin of Environmental Contamination and Toxicology*, Vol. 51, Oct. 1993, pp. 596–599.

[32]Neary, D. G., Bush, P. B., and Michael, J. L., "Fate, Dissipation and Environmental Effects of Pesticides in Southern Forests: A Review of a Decade of Progress," *Environmental Toxicology and Chemistry*, Vol. 12, No. 3, 1993, pp. 411–428.

[33]Dowd, J., Bush, P., Neary, D., and Taylor, J., "Modeling Pesticide Movement in Forested Watersheds: Use of PRZM for Evaluating Pesticide Options in Loblolly Pine Stand Management," *Environmental Toxicology and Chemistry*, Vol. 12, 1993, pp. 429–439.

[34]Nutter, W. L., Knisel, W. G., Jr., Bush, P. B., and Taylor, J. W., "Use of GLEAMS to Predict Insecticide Losses from Pine Seed Orchards," *Environmental Toxicology and Chemistry*, Vol. 12, No. 3, 1993, pp. 429–439.